Precision Magnetic Moment Determinations for 43-min ^{199m}Hg and Other Isomers of Mercury*

R. J. Reimann and M. N. McDermott
University of Washington, Seattle, Washington 98195
(Received 2 January 1973)

Optical pumping with the 2537 Å intercombination line of mercury has been used to orient four nuclear spin $I=\frac{13}{2}$ isomers of mercury and two $I=\frac{1}{2}$ radioisotopes as well as stable $I=\frac{1}{2}$ ^{199}Hg and $I=\frac{3}{2}$ ^{201}Hg. Measurements of ratios of the nuclear-magnetic-resonance frequencies of these isotopes to that of ^{199}Hg contained in the same sample cell have been made. The results are:

Spin	Isotope	Half-life	ν/ν_{199}
$\frac{13}{2}$	193*m*	11 h	0.160 940 9(3)
	195*m*	40 h	0.158 845 2(3)
	197*m*	24 h	0.156 265 9(3)
	199*m*	43 min	0.154 292 0(3)
$\frac{3}{2}$	201	stable	0.369 138 7(7)
$\frac{1}{2}$	195	9.5 h	1.070 350 8(20)
	197	64 h	1.042 477 9(5)

Independent measurements also give $\nu_{195m}/\nu_{195}=0.148\,405\,1(3)$ and $\nu_{197m}/\nu_{197}=0.149\,898\,4(3)$. Values of $A(^3P_1)$ are combined with the above ratios to give differential hyperfine-structure anomalies. Magnetic moments and hyperfine-structure anomalies are calculated by means of a nuclear configuration-mixing model and compared with the experimental results.

I. INTRODUCTION

An extensive series of measurements of the nuclear moments[1-8] and atomic hyperfine structure (hfs)[9-12] of the isotopes and isomers of mercury has been made over the past several years. This work reports on a measurement of the nuclear magnetic moment of a mercury isomer previously not studied by optical-pumping methods, 43-min ^{199m}Hg, as well as precision determinations of the moments of several other mercury isotopes and isomers.

The combination of magnetic moment and atomic hfs measurements has a very interesting aspect in that it provides a test of nuclear models which is sensitive to the spatial distribution of nuclear magnetism. That part of the hfs interaction which arises from the interaction of a valence electron with the nuclear dipole moment of an extended nucleus is reduced from the value which it would have for a nucleus with a point charge, point magnetic dipole moment. If $W_{\rm ext}$ is the hyperfine-interaction energy for the actual, extended nucleus and $W_{\rm pt}$ is the energy expected for a point nucleus with the same dipole moment, then the relation $W_{\rm ext} \equiv W_{\rm pt}(1+\epsilon)$ defines the hyperfine anomaly ϵ.

In practice ϵ is usually not available directly from measurements because present atomic wave functions do not give $W_{\rm pt}$ to sufficient accuracy. If adjacent isotopes are compared, however, the atomic wave functions are very closely the same; and the difference between the anomalies of the two isotopes or the "differential anomaly" $_1\Delta_2=\epsilon_1-\epsilon_2$ is independent of the wave functions. The differential anomaly depends only very slightly on the difference in nuclear charge radius between the two isotopes but is quite sensitive to a change in the relative contribution of spin and orbital magnetism to the nuclear magnetic moments.[13] Differential hfs anomalies are computed in this paper for a substantial number of mercury isotopes and isomers, and the results are compared to predictions for the same quantities based on a nuclear model employing configuration mixing.

The first portion of the paper is devoted to a description of the apparatus and the process of optically pumping mercury with the 2537 Å $(6^3P_1 \rightarrow 6^1S_0)$ intercombination line. This is followed by a discussion of the data reduction and a presentation of the final values of the measurements. In most cases the quantity measured was the ratio of the nuclear resonance frequency of a mercury isotope or isomer to that of ^{199}Hg in the same magnetic field. Preliminary results were presented earlier in abstract form.[14,15]

II. EXPERIMENTAL DETAILS

A. Nuclear Orientation Apparatus

The experimental apparatus is shown schematically in Fig. 1. The optical pumping light was produced by electrodeless discharge lamps. They were excited by a modified 125-W magnetron operating at 2450 MHz and were located in the gap of a 10-cm electromagnet which produced a magnetic "scanning" field $\vec{H}_s$. This field shifted the frequency of the optical radiation by means of the Zeeman effect and could be set to give optimum overlap between the lamp spectral profile and the absorption profile of the isotope being oriented. The light was right or left circularly polarized by a Polacoat UV-105 linear polarizer (47% visible transmittance) and a strained-quartz quarter wave plate. The pumping beam was directed along a static homogeneous magnetic field $\vec{H}_0$ and focused onto the sample cell with quartz lenses.

Cylindrical sample cells were constructed from 25-mm-diam clear fused quartz and were 25 mm long with fused quartz windows on the ends. They were located in the center of the field $\vec{H}_0$ produced by a Helmholtz pair with a mean diameter of 41 cm. This field had a maximum magnitude of about 650 Oe, an rms variation of about 10 ppm over the volume of the cell body, and a time stability of about 5 ppm/h. The cells were raised to temperatures of 300 to 500°C by an electrically heated oven. This was necessary in order to reduce the rate of spin relaxation on the cell walls.

The π and σ polarization components of the light which were reemitted by the sample were monitored with photomultipliers perpendicular to the pumping beam. Visible light was blocked by an absorption filter containing a saturated solution of $NiSO_4$ and $CoSO_4$.[16] The resulting π and σ signals were either measured individually or subtracted in a differential amplifier to give a balanced detection. The signal was sent through a Multimetrics AF-210 low-pass filter and then digitized in a 12-bit Digital Equipment Corporation AF01 analog-to-digital converter. It was finally stored in a PDP 8/I computer operating as a signal averager.

The computer, in turn, swept the frequency output of a Hewlett Packard 5100A/5110A frequency synthesizer by means of a specially constructed digital sweep unit.[17] The frequency was known to better than 1 part in 10^9 through comparison with WWVB and was maintained to better than 3 parts in 10^8. The rf output of the synthesizer was applied to a coil which provided an rf magnetic field $\vec{H}_1$ perpendicular to $\vec{H}_0$. The nuclei, which had been oriented by the transfer of angular momentum from the circularly polarized light, were disoriented as the rf was swept through their Larmor precession frequency. This resulted in a change in the intensity of the π and σ polarization components monitored by the photomultipliers.

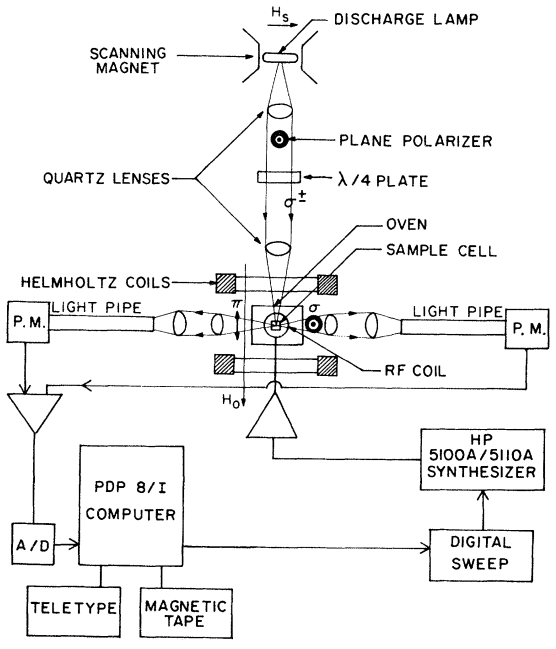

FIG. 1. Schematic diagram of the optical pumping apparatus and associated electronics.

B. Resonance Lamps

The lamps which produced the resonance radiation for optical pumping were a critical element in the success of these measurements. They were made of fused quartz and were shaped roughly like a disk 25 mm in diameter and a few mm thick. Each lamp contained 1 to 2 mg of an enriched mercury isotope and 1 to 2 Torr of argon buffer gas.

As is apparent from Fig. 2 the hyperfine components of the 2537 Å line are separated by many times the Doppler width. For this reason it is necessary to select an isotope with a component overlapping a component of the isotope to be pumped or to shift the spectrum of the lamp by means of an applied magnetic field. The "scanning field" H_s and a suitable isotope for the lamp can be selected by referring to Fig. 2. This plot of mercury hyperfine-level structure is based on the summary of Tomlinson and Stroke.[18] The levels for ^{193}Hg were taken from the later work of Fulop *et al.*[19] and those for ^{199m}Hg from that of Covey and Davis.[20]

The following example illustrates the method of selection. Suppose that one desires to pump both ^{193m}Hg and ^{199}Hg with a single setting of H_s. As shown in Fig. 2, this can be accomplished by using

an enriched ^{202}Hg lamp in a field which splits the $m_J = \pm 1$ levels of the $^3P_1$ state by ±4.9 GHz. For mercury these levels split from the center of gravity of the unshifted line at the rate of ±2.077 MHz/Oe. The component originating from the $m_J = 0$ sublevel is not shown. It is unshifted by the mag-

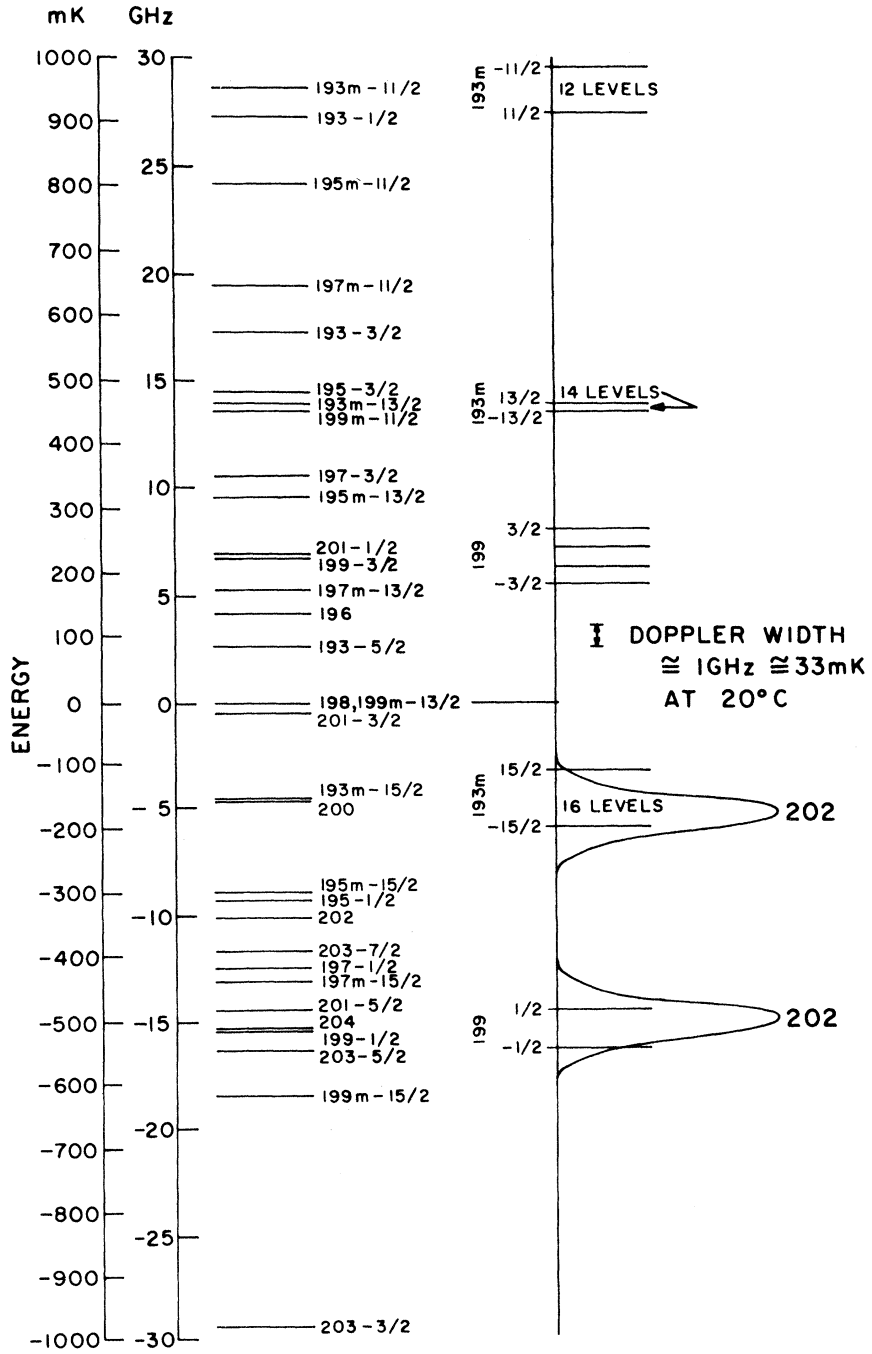

FIG. 2. Hyperfine components of the 2537-Å mercury intercombination line. On the right-hand side of the figure, the spectrum expected from a ^{202}Hg lamp operated in a magnetic field $H_s = 2400$ Oe is superimposed on the hyperfine components expected for ^{193m}Hg and ^{199}Hg in a field $H_0 = 650$ Oe. The lamp spectrum is drawn as two Gaussian-shaped lines with the widths measured in this research. The lamp spectrum is the one which would be observed at right angles to the field $\vec{H}_s$ through a polarizer set to pass only light linearly polarized perpendicular to the field.

TABLE I. Summary of results for nuclear-resonance frequency ratios.

Isotopes pumped	Lamp isotope	Scanning field (GHz)	hfs Component pumped	Polarization pumping/detection (filters)	Number of ratios	Frequency ratios [a]
193m/199	202	4.9	$F=\frac{15}{2}$, $F=\frac{1}{2}$	σ^+/σ	4	0.160 941 00 (13) [b]
	202	4.9	$\frac{15}{2}$ $\frac{1}{2}$	σ^+/b	4	0.160 940 84 (9)
	198	5.4	$\frac{15}{2}$ $\frac{3}{2}$	$\sigma^-, \sigma^+/b$	2	0.160 940 89 (16) $\langle 0.160\,940\,92\ (8)\rangle_{av}$
195/199	202, 204	0	$\frac{1}{2}$ $\frac{1}{2}$	σ^-/π (46%)	4	1.070 350 8 (5)
	202, 204	0	$\frac{1}{2}$ $\frac{1}{2}$	σ^-/σ (46%)	4	1.070 350 8 (5) $\langle 1.070\,350\,8\ (3)\rangle_{av}$
195m/195	202	0	$\frac{15}{2}$ $\frac{1}{2}$	σ^-/π	15	0.148 405 17 (5)
	198	8.3	$\frac{15}{2}, \frac{13}{2}$ $\frac{1}{2}$	σ^+/σ	3	0.148 404 65 (10) $\langle 0.148\,405\,08\ (7)\rangle_{av}$
195m/199	Natural	0	$\frac{15}{2}$ $\frac{3}{2}, \frac{1}{2}$	σ^-/π	5	0.158 845 44 (10)
	Natural	0	$\frac{15}{2}$ $\frac{3}{2}, \frac{1}{2}$	$\sigma^-, \sigma^+/\pi$	4	0.158 844 91 (12)
	198	7.5	$\frac{15}{2}$ $\frac{3}{2}$	σ^-/π	7	0.158 844 96 (11)
	202, 204	0	$\frac{15}{2}$ $\frac{1}{2}$	σ^+/π (46%)	7	0.158 845 22 (16)
	202, 204	0	$\frac{15}{2}$ $\frac{1}{2}$	σ^-/π (46%)	4	0.158 845 56 (19)
	202, 204	0	$\frac{15}{2}$ $\frac{1}{2}$	σ^-/π	2	0.158 845 70 (16) $\langle 0.158\,845\,23\ (7)\rangle_{av}$
197/199	202, 204	0	$\frac{1}{2}$ $\frac{1}{2}$	σ^+/π (46%)	5	1.042 479 03 (21)
	202, 204	0	$\frac{1}{2}$ $\frac{1}{2}$	σ^+/π	5	1.042 480 36 (39)
	202, 204	0	$\frac{1}{2}$ $\frac{1}{2}$	σ^-/π	4	1.042 480 58 (17) $\langle 1.042\,477\,9\ (5)\rangle_{extrap.}$ [c]
197m/197	202	3.4	$\frac{15}{2}$ $\frac{1}{2}$	σ^-/π	2	0.149 898 31 (15)
	198	12.7	$\frac{15}{2}$ $\frac{1}{2}, \frac{3}{2}$	σ^+/b	5	0.149 898 32 (14)
	198	12.9	$\frac{15}{2}$ $\frac{1}{2}, \frac{3}{2}$	σ^+/π	3	0.149 898 61 (8)
	198	12.9	$\frac{15}{2}$ $\frac{1}{2}, \frac{3}{2}$	σ^-/σ	3	0.149 898 25 (6)
	198	12.9	$\frac{15}{2}$ $\frac{1}{2}, \frac{3}{2}$	σ^-/σ	3	0.149 898 37 (12) [d]
	198	12.9	$\frac{15}{2}$ $\frac{1}{2}, \frac{3}{2}$	σ^-/b	3	0.149 898 09 (10) [d]
	198	12.9	$\frac{15}{2}$ $\frac{1}{2}, \frac{3}{2}$	σ^+/b	3	0.149 899 00 (8) [d] $\langle 0.149\,898\,42\ (7)\rangle_{av}$
197m/199	202	3.4	$\frac{15}{2}$ $\frac{1}{2}$	σ^+/π	8	0.156 265 95 (13)
	202	3.4	$\frac{15}{2}$ $\frac{1}{2}$	σ^+/π (64%)	6	0.156 265 81 (27)
	202	3.4	$\frac{15}{2}$ $\frac{1}{2}$	σ^+/π	13	0.156 266 13 (16)
	198	17.1	$\frac{11}{2}$ $\frac{1}{2}$	σ^-/π	4	0.156 266 00 (6)
	198	16.9	$\frac{11}{2}$ $\frac{1}{2}$	σ^-/π	3	0.156 265 74 (17)
	198	16.9	$\frac{11}{2}$ $\frac{1}{2}$	σ^-/σ	3	0.156 265 86 (5)
	198	16.9	$\frac{11}{2}$ $\frac{1}{2}$	σ^-/σ (46%)	5	0.156 265 77 (6) $\langle 0.156\,265\,95\ (7)\rangle_{av}$
199m/199	198	14.9	$\frac{11}{2}$ $\frac{1}{2}$	σ^+/b	3	$\langle 0.154\,292\,04\ (12)\rangle_{av}$
201/199	198	6.9	$\frac{1}{2}$ $\frac{3}{2}$	σ^-/π	5	0.369 138 80 (9)
	198	14.9	$\frac{5}{2}$ $\frac{1}{2}$	σ^+/π	4	0.369 138 31 (15)
	198	6.9	$\frac{1}{2}$ $\frac{3}{2}$	σ^-/b	5	0.369 138 98 (16) $\langle 0.369\,138\,72\ (11)\rangle_{av}$

[a] Except as noted the ratios were obtained in a magnetic field $H_0 \approx 650$ Oe.
[b] Uncertainties are 1σ in the unweighted means except for 199m/199 where a weighted mean is used.
[c] The ratio obtained by a linear extrapolation of the first two sets of ratios to the zero light intensity value.
[d] $H_0 \approx 320$ Oe.

netic field but in these experiments was absorbed from the pumping beam by a linear polarizer set with its pass axis perpendicular to the field. The levels of ^{193m}Hg and ^{199}Hg are shown with Zeeman splittings appropriate to $H_0 = 650$ Oe. The lamp profile is shown with a Gaussian shape and widths of 2.0 GHz. This width is in agreement with measurements made by orienting ^{199}Hg with an even-isotope lamp and noting the dependence of the resonance amplitude on the scanning field. The widths found are twice the Doppler width at 20°C. The selection of lamps and scanning fields used for each isotope is given later in Table I.

Optical pumping through the $F = \frac{11}{2}$ and $F = \frac{1}{2}$ hyperfine levels for the respective $I = \frac{13}{2}$ and $I = \frac{1}{2}$ isomers was more efficient than through $F = \frac{15}{2}$ and $F = \frac{3}{2}$. Attempts to use $F = \frac{13}{2}$ were unsuccessful. This may have been due to an imperfect circular polarizer and the small Zeeman splitting. The latter would minimize any intensity pumping caused by unequal illumination of the sublevels.

C. Isotope Production

The radioactive mercury isotopes were prepared at the University of Washington 60-in. cyclotron. The first experiments were performed on ^{197}Hg and ^{197m}Hg produced by the reaction ^{197}Au$(d, 2n)^{197, 197m}$Hg. The 21-MeV deuterons were degraded by a $10 \times 2 \times 0.013$-cm-thick commercially pure gold target foil to about 15 MeV.[21] That is the energy at which the cross section for ^{197m}Hg production peaks at almost 300 mb and below which the cross section for ^{197}Hg predominates.[22] A beam current of 25 μA incident for 4 h produced sufficient ^{197}Hg and ^{197m}Hg to give good optical-pumping signals. An average reaction cross section of about 280 mb for each isotope predicts that roughly 3×10^{13} atoms of each were produced.

The mercury activity was distilled from the target foils under vacuum with an induction heater and was trapped in a silvered[23] U tube immersed in a dry-ice–trichlorethylene slush. It was then distilled under high vacuum into sample cells which had been prefilled with approximately 5×10^{13} atoms of ^{199}Hg to serve as a reference. The cells were finally sealed off leaving short tails of the 1-mm capillary through which they had been filled.

Additional mercury isotopes were later produced by the bombardment of commercially pure natural platinum foils with α particles. The main production reaction was ^{A}Pt$(\alpha, 3n)^{A+1}$Hg. Lange and Münzel[24] predict a 1000-mb cross section for this reaction which peaks at $E + Q = 11$ MeV and has a Maxwellian shape and full width at half maximum of 12 MeV. The various reaction Q values may be calculated from the recent mass-excess values of Wapstra and Gove.[25] For the production of ^{199m}Hg, this suggests a combination of 0.005 cm of aluminum used to degrade the 42-MeV α beam to 40 MeV followed by a 0.008-cm-thick platinum target foil. Bombardments of 30–35 μA were made for 3 h, roughly 3 mean lives of ^{199m}Hg. Sufficient ^{199}Hg was also produced to provide good reference signals so that it was unnecessary to prefill these cells.

Finally, it should be mentioned that the reaction ^{197}Au$(\alpha, pn)^{199, 199m}$Hg was also used but with less success due to the smaller, 30-mb cross section. The production of ^{198}Tl and ^{199}Tl also tripled the radiation hazard.

D. Signal-Averaging Procedure

The signal-averaging program was a direct-sum averager which accumulated the digitized voltage readings in a storage buffer composed of sequentially addressed memory locations. Each of these locations is hereafter referred to as a "channel." After initially zeroing the storage buffer, the operating sequence was: (1) Digitize the dc signal, (2) add the results in double precision to the contents of channel one, (3) send a preselected number of pulses to change the rf frequency, and (4) advance to the next channel; whereupon the sequence was repeated. After making entries into all of the desired channels (512 max), return was made to channel one and the accumulation continued until manually interrupted at the end of any pass. The final accumulated results were stored on magnetic tape and later recalled for analysis.

The digital sweep unit was designed to sweep any three consecutive decades of the synthesizer. An increment of 1 in the lowest selected decade was made each time a pulse was received. The upper and lower limits of the sweep were preselected on the sweep unit which automatically reversed upon reaching them. The resulting rf field sweep was kept in phase with the computer storage channels by proper selection of the sweep limits, total number of storage channels, and number of pulses generated for each channel. The synthesizer was swept both up and down through the resonance frequency for each pass of the averaging program in order to correct for apparent shifts of the resonance frequency due to finite system-response times. Since the synthesizer reversal occurred at the middle of a computer pass the "up" and "down" resonances were stored separately.

In order to minimize distortion of the signal line shapes, the sweep time was kept much longer than the spin system response time. Also, the high-frequency cutoff of the filter was kept higher than the channel switching rate. Typical sweep times

through a frequency interval equal to approximately 4 linewidths of the resonances were 10 and 40 sec for the $I=\frac{1}{2}$ and $\frac{13}{2}$ isomers, respectively. The respective high-frequency cutoffs were typically 30 and 3 Hz for about 100 channels per resonance or 5 and 0.5 Hz for about 25 channels per resonance.

III. RESULTS

A. Data Analysis

The data in digital form were analyzed by fitting a theoretical line shape to each of the accumulated resonance signals. In the limit of low rf magnetic fields the line shape which should be observed is Lorentzian even for the spin $I=\frac{13}{2}$ isomers. In higher fields the shape may depart from a Lorentzian, but it is still expected to be symmetric about a frequency $\nu_0=(1/2\pi)\gamma H_0$, where γ is the nuclear gyromagnetic ratio and H_0 is the static field. As a consequence the center of any fitted symmetric curve should coincide with the desired center frequency ν_0.

In practice the form usually assumed for the accumulated signal $f(x_i)$ as a function of the channel

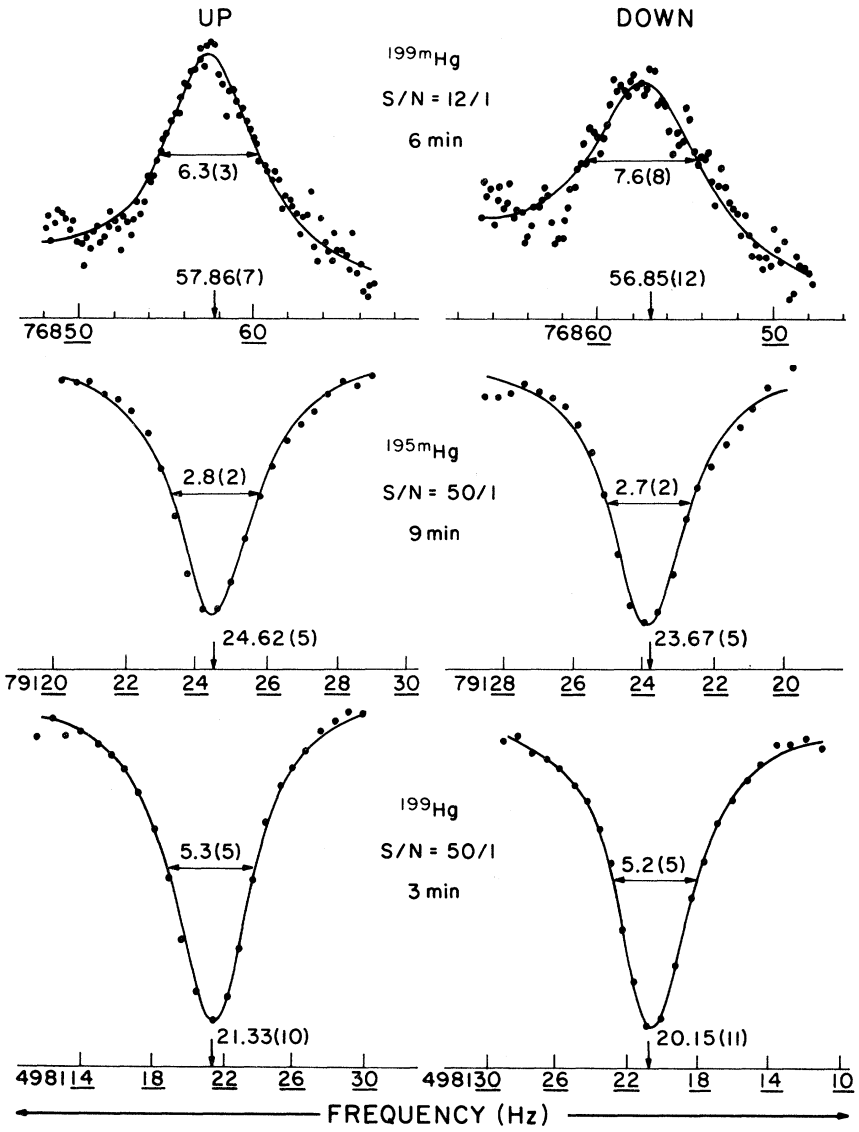

FIG. 3. Nuclear resonance signals observed for ^{199m}Hg, ^{195m}Hg, and ^{199}Hg. The dots are the experimental points and the solid curves are least-squares fitted theoretical line shapes. Indicated on the diagram are the resonance centers for signals obtained with frequency increasing as a function of time, "up", and decreasing "down"; the full linewidth at half maximum; the signal to noise ratio; and the total time taken to acquire both "up" and "down" resonances.

number x_i was $f(x_i) = A(W/2)^2/[(W/2)^2 + (x_i - x_0)^2] + B$. The parameters obtained from fitting this function to the data were: x_0, the resonance center; W, the full width at half maximum; A, the signal amplitude; and B, the assumed constant background signal. For ^{199m}Hg only, a term Cx_i was added to allow for a slope in the background signal. The fitting procedure, carried out by means of a FOCAL program on the PDP 8/I, minimized the quantity $Q = \sum_i [Y(x_i) - f(x_i; x_0, W, A, B)]^2 w_i$. $Y(x_i)$ is the observed signal and w_i the weight for the ith channel. $w_i = 1/\sigma_i^2$ where σ_i is the standard deviation of the signals accumulated in the ith channel. Experience demonstrated that σ_i was nearly the same for all channels as would be expected for a noise source consisting largely of photomultiplier shot noise and lamp noise. Consequently, σ_i was determined by computing the rms fluctuation of the data points in the wings of the resonance. The fitting routine followed that described by Ehlers *et al.*[26] and yielded, in addition to the best-fit parameters x_0, W, A, and B, the standard errors of the parameters and the value of χ^2 for the fit.

Several signals and the fitted resonance curves are shown in Fig. 3. In each case the first signal was obtained with the frequency increasing as a function of time ("up" resonance) and the second with it decreasing ("down" resonance). The values of x_0 and W (converted to frequency units from the known correspondence between channel and frequency) and the signal to noise ratio $S/N = A/\sigma_i$ are indicated for each resonance.

The standard errors of the parameters shown in Fig. 3 are typical of those obtained for the given isotopes throughout this study. In particular the values of χ^2/(degrees of freedom) were about 1. This tends to show that the line shape was Lorentzian and supports the interpretation of the line center as the frequency corresponding to $\nu_0 = (1/2\pi)\gamma H_0$. The small displacements which occur as a result of finite system-response time and finite sweep rate are removed to an accuracy exceeding the quoted uncertainty in an individual line center by the procedure of averaging the center frequencies of the "up" and "down" resonances.

The averaged resonance frequencies for a given isomer as well as those for the comparison isotope were plotted as a function of the time the resonances were acquired. An example of such a plot, in this case for ^{195m}Hg, is shown in Fig. 4. The ratio of the isomer frequency to that expected for ^{199}Hg at the same time was obtained by a linear interpolation of the ^{199}Hg frequency between resonances acquired just before and just after the isomer signal. This procedure should eliminate the effect of steady drifts in the magnetic field.

The prinicpal source of scatter in the data was fluctuation in the magnetic field. As indicated in Fig. 4 field drifts of ~5 ppm/h and shorter term fluctuations of ~2 ppm were encountered. For all isotopes and isomers the standard error in an individual ratio determination averaged about 1.3 ppm. This indicates rms field fluctuations of this magnitude over the time needed to measure a resonance pair.

B. Ratio Measurements and Light-Shift Corrections

The results of all sets of ratio measurements are contained in the last column of Table I. Also included for each set are: (1) the isotope(s) used in the lamp, (2) the scanning field, (3) the hfs level in the $^3P_1$ state through which most of the pumping occurred, (4) the polarization of the pumping light (σ^+ or σ^-) and the polarization of the scattered light detected (σ, π, or b – balanced detection), and (5) the number of resonance pairs in the set. All the measurements in Table I with the exceptions noted were carried out in a field of about 650 Oe, nearly the maximum available.

As has been demonstrated both theoretically and experimentally by Cohen-Tannoudji[27, 28] the pumping light can cause shifts in the ground-state resonance frequency. Under special circumstances shifts as large as 6 Hz have been produced in the ^{199}Hg resonance.[29]

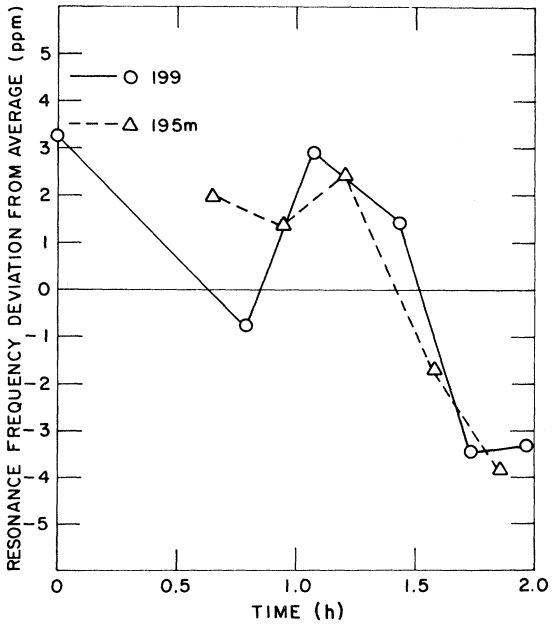

FIG. 4. Nuclear resonance frequency deviations for ^{195m}Hg and ^{199}Hg as a function of time.

Light shifts are usually attributed to "real" transitions, which arise from portions of the lamp spectrum resonant with the optical transition, and "virtual" transitions which arise from off-resonant light. In the present experiment shifts due to real transitions are negligibly small. Although the theory for such shifts has not been worked out in detail for the spin $I=\frac{13}{2}$ isomers, the shifts depend, in all cases, on a near coincidence between transition frequencies in the excited states involved in the pumping and the transition frequency in the ground state. In a field of 650 Oe, ground-state frequencies of 80 to 500 kHz differ from the 200-MHz Zeeman frequencies in the excited state by many times the excited-state decay frequency, $\Gamma=9\times10^{6}\ \mathrm{sec}^{-1}$.

Shifts due to virtual transitions are a more serious problem. In these experiments scanning field settings were chosen so that the lamp spectrum would simultaneously overlap hyperfine components of both the reference isotope and the chosen isomer. This sometimes resulted in a lamp spectrum displaced from the absorption spectra by amounts on the order of a Doppler width. Despite the fact that this procedure invited light shifts, such compromise settings were preferable to changing the scanning field back and forth between values suitable first for the reference isotope and then for an isomer. The latter procedure was undesirable because the scanning magnet produced a small fringing field at the positon of the absorption cell which was neither easily measured nor precisely reproducible. The resulting uncertainties would have been larger than those due to the light shifts.

Corrections for light shifts based on theory were out of the question on several grounds. Firstly, a calculation requires a knowledge of the spectral profile of the lamp as well as its absolute intensity. Neither quantity was well known. Secondly, the elegant theory of Happer and Mathur,[30] which gives values for these shifts in terms of a fictitious magnetic field and a fictitious electric-field gradient, cannot be used since it assumes that the separation between Zeeman sublevels is small compared to the spectral width of the lamp, a situation which is not true for mercury in a 650-Oe field. Although magnitudes of shifts could not be calculated their signs could be inferred with reasonable certainty in most cases.

Accordingly, attempts were made to measure and correct for light shifts empirically. The useful fact about light shifts, which can be exploited in a measurement, is that they are expected to be proportional to the incident-light intensity in all cases. An auxilliary experiment was, therefore, conducted with ^{197m}Hg in which a series of neutral-density filters (perforated screens) were placed in sequence in the pumping-light beam and the resonance frequency observed for each filter value. The sequence of measurements was repeated several times in order to correct for field fluctuations. For this experiment a ^{202}Hg lamp was used in three different scanning fields, $H_s=3.2$, 3.8, and 4.7 GHz. The polarization of the pumping light was σ^+ in all cases. The positions of the lamp components relative to the ^{197m}Hg hfs are shown in Fig. 5. The spectral width as drawn is twice the Doppler width at 20°C. For $H_s=3.2$ and 3.8 GHz the data are consistent with zero light shift to within 1 ppm. For $H_s=4.7$ GHz a shift of $-1.4(7)$ ppm is found. That the lamp spectrum for $H_s=4.7$ GHz was substantially off resonance is attested to by the fact that the resonance signal was broadened by the light only very slightly compared to resonances obtained at the other two scanning fields.

Although this measurement on ^{197m}Hg with one type of lamp cannot be used to infer light shifts for other isotopes and lamps it does serve to indicate the magnitude expected for such shifts. The ^{202}Hg lamp used was exceptionally bright and the scanning field was adjusted to give a maximum shift (higher fields resulted in greatly reduced pumping rates and, consequently, reduced signals). On this basis it is assumed that the light shifts en-

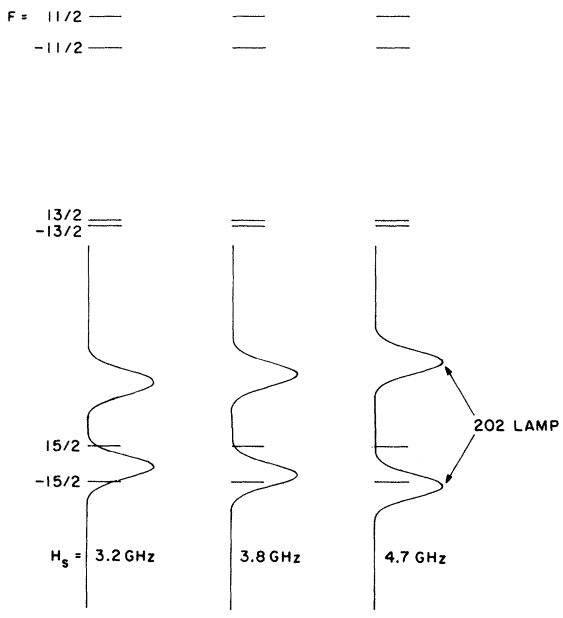

FIG. 5. Overlap between the spectrum of a ^{202}Hg lamp operated in various magnetic fields and the hyperfine components of ^{197m}Hg in a field of 650 Oe. The lamp spectrum is taken to have a Gaussian shape with a full width at half maximum of 2 GHz.

countered in the mercury isomers did not greatly exceed 1 ppm.

For most of the ratio measurements several different lamps, scanning fields, and light polarization choices were made. In a few instances neutral-density filters were also employed. With the sole exception of the ν_{197}/ν_{199} ratio the results were consistent with zero light shift in the ratios to within about 1 ppm. The ν_{197}/ν_{199} ratio shift obtained from the data is −2.3(6) ppm. Since both isotopes have spin $I=\frac{1}{2}$ the theory of the shift is much simpler and less ambiguous than for the $I=\frac{13}{2}$ isomers. With the ^{202}Hg-^{204}Hg mixture used in the lamp the shifts seen in ^{197}Hg and ^{199}Hg resonances are expected to be opposite in sign, thus increasing the shift in the frequency ratio over that for an individual resonance. In this case the value of the ratio extrapolated to zero light intensity is quoted as the proper unshifted value. In all other cases the data from runs taken under different conditions are lumped together and treated as belonging to the same parent distribution. The uncertainty quoted in the final column of Table I is thus the standard error in the unweighted mean of all the data taken for a given isotope pair with the exception of that for the pair 197/199, where it is the standard error in the extrapolated value of the ratio.

In view of the limited experimental information on light shifts the standard errors quoted in Table I should not be considered to be the standard errors in the unshifted ratio values. The final set of values given in Table II is arbitrarily assigned an uncertainty of ±2 ppm. The data on ^{197m}Hg and the internal consistency of the data for each isotope pair give confidence that the true values will likely be contained within this limit. Other possible sources of systematic error have been carefully investigated and none make a significant addition to the 2 ppm uncertainty adopted.

TABLE II. Final values of nuclear resonance frequency ratios.

Ratio	This work	Previous measurements
ν_{193m}/ν_{199}	0.160 940 9 (3) [a]	0.160 933 (18) [b]
ν_{195}/ν_{199}	1.070 350 8 (20)	1.070 356 (66) [c]
ν_{195m}/ν_{195}	0.148 405 1 (3)	
ν_{195m}/ν_{199}	0.158 845 2 (3)	0.158 832 (10) [b]
ν_{197}/ν_{199}	1.042 477 9 (5)	1.042 479 (15) [d]
ν_{197m}/ν_{197}	0.149 898 4 (3)	
ν_{197m}/ν_{199}	0.156 265 9 (3)	0.156 234 (12) [b]
ν_{199m}/ν_{199}	0.154 292 0 (3)	
ν_{201}/ν_{199}	0.369 138 7 (7)	0.369 138 80 (15) [e]

[a] The quoted uncertainty for all ratios except ν_{197}/ν_{199} is 2 ppm and represents the authors' estimate of the magnitude of possible systematic errors arising from light shifts. The uncertainty for ν_{197}/ν_{199} is 1σ in the ratio extrapolated to its zero light intensity value. Reference b uncertainties are 1σ, the others are stated to be 3σ.

[b] Reference 7.

[c] W. T. Walter and M. J. Stavn, Bull. Am. Phys. Soc. 9, 10 (1965).

[d] W. T. Walter, Bull. Am. Phys. Soc. 7, 295 (1962).

[e] Reference 4.

The results of our measurements are in excellent agreement with earlier measurements where they are available. In the one instance of a previous measurement of higher precision,[5] that for ν_{199}/ν_{201}, the authors took considerable care to avoid light shifts. The agreement with their result certainly precludes light shifts in the present data at the claimed 2-ppm level.

A further check of the internal consistency of the data is possible. The data from Table I give a value for $[\nu_{197m}/\nu_{197}][\nu_{197}/\nu_{199}]=0.156\,265\,79(10)$ which compares well with the independent value $\nu_{197m}/\nu_{199}=0.156\,265\,95(7)$ from the same table. Likewise $[\nu_{195m}/\nu_{195}][\nu_{195}/\nu_{199}]=0.158\,845\,50(9)$ is to be compared with $\nu_{195m}/\nu_{199}=0.158\,845\,23(7)$, an agreement within 2 ppm.

C. Nuclear Magnetic Moments

The ratio of the nuclear magnetic moments is obtained directly from the measured nuclear resonance frequencies and the nuclear spins, $\mu_1/\mu_2=(\nu_1/\nu_2)(I_2/I_1)$. The nuclear moments in nuclear magnetons, uncorrected for diamagnetic shielding in the mercury atom, follow from the earlier results $\mu_{199}/\mu_p(H_2O)=+0.178\,270\,6(3)$[1] and $\mu_p(H_2O)/\mu_N=2.792\,774(2)$.[31] The moments thus obtained are given in Table III.

The most recent calculations of the diamagnetic correction[32] in mercury give 1.016 13 as the factor by which the bare nuclear moment exceeds the shielded value. Since the authors do not assign an uncertainty to their result it is arbitrarily taken to be 5% of the correction. The resulting moments are also given in Table III.

TABLE III. Nuclear magnetic moments.

Isotope	μ/μ_N uncorrected	μ/μ_N (with diamagnetic correction) [a]
193m	−1.041 658 (3)	−1.058 5 (8)
195	+0.532 894 6 (13)	+0.541 5 (4)
195m	−1.028 094 (3)	−1.044 7 (8)
197	+0.519 017 9 (8)	+0.527 4 (4)
197m	−1.011 401 (3)	−1.027 7 (8)
199m	−0.998 624 (3)	−1.014 7 (8)

[a] The diamagnetic correction is taken to be $1/(1-\sigma)=1.016\,13\,(80)$. See Reference 32.

D. Differential hfs Anomalies

The frequency ratios given above can be combined with previous measurements of the hfs of the $^3P_1$ state to give differential hfs anomalies. The differential anomaly for the $^3P_1$ state is defined to be $_1\Delta_2(^3P_1) = [A_1(^3P_1)]/[A_2(^3P_1)]\ g_2/g_1 - 1$, where $A(^3P_1)$ is the magnetic-dipole interaction constant for this state and g is the nuclear g factor. The subscripts refer to the two isotopes being compared with the subscript 1 usually designating the lighter isotope. The ratio $g_2/g_1 = \nu_2/\nu_1$, the nuclear resonance frequency ratio, and is thus given in Table II. The appropriate $A(^3P_1)$ values are summarized in Table IV as are the calculated anomalies. The dipole constants were obtained from earlier level crossing and double resonance measurements as indicated, although the values given differ slightly from those quoted by the authors. Their measured level-crossing fields and hyperfine frequencies were used[33] to find the $A(^3P_1)$ values in a consistent program which included the perturbation of the $^3P_2$, $^3P_0$, and $^1P_1$ states to second order[34] and a correction for the different radial dependence of the p electron in the singlet and triplet states.[35] The constants employed are listed in Table V.

In comparing the anomaly to theory it is more useful to have the anomaly for the s electron alone, $_1\Delta_2(s_{1/2})$. This can be obtained from $_1\Delta_2(^3P_1)$ and a simple extension of Lurio's[35] results. For example,

$$A_{201}(^3P_1)\,{}_{199}\Delta_{201}(^3P_1) = \left(\frac{\alpha^2}{4} - \frac{\sqrt{2}}{2}\,\alpha\beta\right) a_s(201)\,{}_{199}\Delta_{201}(s_{1/2}) + \left(\frac{\alpha^2}{3} - \frac{\sqrt{2}}{3}\,\alpha\beta\lambda + \frac{\beta^2\lambda^2}{6}\right) a_{1/2}(201)\,{}_{199}\Delta_{201}(p_{1/2}), \quad (1)$$

where it has been assumed that the anomaly for the $p_{3/2}$ electron, $_{199}\Delta_{201}(p_{3/2})$, and for the off-diagonal $p_{1/2,3/2}$ term, $_{199}\Delta_{201}(p_{1/2,3/2})$, are both zero. α and β are the triplet and singlet amplitudes in the nominal $^3P_1$ state. $a_s(201)$ and $a_{1/2}(201)$ are the individual electron magnetic dipole hfs constants. λ is the ratio $\langle S|(1/r^3)|T\rangle/\langle T|(1/r^3)|T\rangle$, where S and T refer to the singlet and triplet states. Values for these constants are listed in Table V. The notation is that of Ref. 34.

The $p_{1/2}$ electron anomaly is not negligible for mercury and can be obtained by first evaluating the s-electron anomaly from the anomaly for the $^3P_2$ state,[36] $_{199}\Delta_{201}(^3P_2) = -0.156\,53(4)\%$, by means of the expression[36] $A_{201}(^3P_2)\,{}_{199}\Delta_{201}(^3P_2) = (\frac{1}{4})a_s(201) \times {}_{199}\Delta_{201}(s_{1/2})$. The result is $_{199}\Delta_{201}(s_{1/2}) = -0.1627(5)\%$. This value, used together with $_{199}\Delta_{201}(^3P_1) = -0.1466(5)\%$ from Table IV, gives $_{199}\Delta_{201}(p_{1/2}) = 0.049(7)\%$. This value seems quite reasonable. The ratio $_{199}\Delta_{201}(p_{1/2})/{}_{199}\Delta_{201}(s_{1/2}) = 0.32(5)$ whereas the work of Stroke, Blin-Stoyle, and Jaccarino[37] predicts 0.23 for this ratio. The ratio of p- to s-electron anomalies should be nearly the same for all pairs of isotopes. If this ratio is chosen to be the experimental value 0.32, then Eq. (1)

TABLE IV. Differential hfs anomalies. The magnetic dipole constants $A(^3P_1)$ have been reevaluated from the original level-crossing or double-resonance measurements according to the results of Lurio (Ref. 35).

Nuclear spin	Isotope (x)	$A(^3P_1)$ (MHz)	$_x\Delta_{199}(^3P_1)$ (%)	$_x\Delta_{199}(s_{1/2})$ (%)
$\frac{1}{2}$	195	15 815.32 (11) [a]	+0.1470 (9)	+0.1630 (20)
	197	15 392.83 (7) [b]	+0.0778 (7)	+0.0862 (12)
	199	14 754.14 (7) [b]	...	
$\frac{3}{2}$	193	−6138.5 (2) [c]	+0.61 (3) [d]	+0.68 (3)
	201	−5454.317 (3) [e]	+0.1467 (6)	+0.1627 (19)
$\frac{5}{2}$	203	4991.33 (4) [f]	+0.796 (16) [g]	+0.883 (20)
$\frac{13}{2}$	193m	−2399.60 (3) [a, c]	+1.0552 (13)	+1.170 (13)
	195m	−2367.96 (8) [a]	+1.038 (3)	+1.151 (13)
	197m	−2329.10 (6) [h]	+1.021 (3)	+1.32 (11)
	199m	−2298.3 (2) [i]	+0.960 (9)	+1.065 (15)

[a] Reference 11.

[b] Reference 10.

[c] O. Redi and H. H. Stroke, Bull. Am. Phys. Soc. 10, 456 (1965); also private communication from Stroke.

[d] The result $\nu_{193}/\nu_{199} = 0.413\,519(40)$ from Moskowitz *et al.* Ref. 7, p. 630.

[e] Reference 9.

[f] Reference 12.

[g] The result $\nu_{201}/\nu_{203} = 1.099\,84\ (18)$ from O. Redi, Ref. 6, p. 567.

[h] Unpublished result obtained in this laboratory. See also, H. R. Hirsch, J. Opt. Soc. Am. 51, 1192 (1961).

[i] R. J. Reimann, B. D. Geelhood, and M. N. McDermott, Bull. Am. Phys. Soc. 16, 848 (1971).

TABLE V. Constants used in the evaluation of second-order hyperfine corrections and hyperfine anomaly reduction.

$g_J(^3P_1)$	$-1.486\,105\ (8)$
α	0.9852 (5)
β	−0.1713 (29)
ξ	1.094
η	1.354
$a_{1/2}/a_{3/2}$	11.83 (60)
λ	0.757 70 (10)
$a_s(201)$	−12 900 (40) MHz
$a_{1/2}(201)$	−2000 (160) MHz

gives $\Delta(s_{1/2}) = 1.109(12)\Delta(^3P_1)$, a result nearly correct regardless of the mercury isotopes compared. The s-electron anomalies obtained are listed in Table IV.

IV. DISCUSSION

A. Configuration-Mixing Model

A nuclear model which has been used to predict successfully the nuclear magnetic moments and hfs anomalies of a wide range of nuclei is the configuration-mixing model of Arima and Horie.[38] A study was undertaken, therefore, to determine to what extent the magnetic moments and anomalies for the mercury isotopes could be computed in a consistent way within the framework of this model.

Arima and Horie and later Noya, Arima, and Horie[39] (NAH) use first-order perturbation theory to obtain a correction to the magnetic moments predicted by a single-particle shell model of the nucleus. They assume a residual two-body interaction V_{12} in addition to a square well or harmonic-oscillator collective potential. V_{12} is taken to be a δ-function interaction between the nucleons. The ratio of the triplet to singlet strengths is chosen to be $V_t/V_s = 1.5$ and V_s is determined empirically from nucleon pairing energies. V_s is related to the neutron-pairing energy P and is parametrized in the theory by a pairing-strength parameter $C = P(j)/[(j+\frac{1}{2})f(nl^2, nl^2)A^{-1/2}]$. $f(nl^2, nl^2)$ is an integral tabulated in NAH, j is the total nuclear angular momentum, and A is the nuclear mass number. The only admixed states which give a correction to the magnetic moment which is linear in the admixed state amplitudes are those which have the same orbital angular momentum as the ground state and have a total angular momentum which differs from it by ±1 unit of angular momentum. This gives rise to the selection rules $\Delta l = 0$ and $\Delta j = \pm 1$ for those admixed states which contribute a correction to the moment. NAH estimate that correction arising from second-order and higher terms in the perturbation theory is less than $0.3\mu_N$.

More recently Stroke, Blin-Stoyle, and Jaccarino[37] have used the configuration-mixing model to compute the hfs anomaly. They obtained electron radial wave functions $f(r)$ and $g(r)$ from a series solution of the Dirac equation. Nuclear single-particle radial wave functions and energies were calculated for a Woods-Saxon potential. Because of the presence of a spin asymmetry operator in the expression for the anomaly, configurations which satisfy the selection rule $\Delta l = \pm 2$ contribute to the anomaly whereas they do not contribute to the moments. On the other hand, the $\Delta l = \pm 2$ contributions to ϵ are usually small, and in the case of the mercury isotopes are estimated to give about 2% corrections.

B. Magnetic Moment and hfs Anomaly Predictions

Two basic parameters are available in attempting to fit moments and anomalies. The first is the choice of a ground-state configuration and the second is the magnitude of the pairing-strength parameter C. Both choices are constrained somewhat. The configuration must give the observed ground-state spin and be consistent with the general order of filling of nuclear levels. The values of C should not differ greatly from those based on the observed pairing energies.

Because the protons form a closed shell at magic number 82, it is reasonable to assume that the correct proton configuration is $\pi(1h_{11/2})^{12}(2d_{3/2})^4(3s_{1/2})^0$. The basic problem, then, is to determine the occupation numbers of the neutron levels for the nuclear ground states and isomeric states of the mercury isotopes so that consistent predictions for μ and ϵ can be made. The neutron number ranges from $N = 113$ to 123 for the isotopes considered, and in this range $1i_{13/2}$, $3p_{3/2}$, $2f_{5/2}$, and $3p_{1/2}$ lie close in energy and compete in the order of filling. For this reason the configurations considered are those of the set $\nu(1i_{13/2})^w(3p_{3/2})^x(2f_{5/2})^y(3p_{1/2})^z$, where $w+x+y+z = N-100$. The exact spacings between levels of

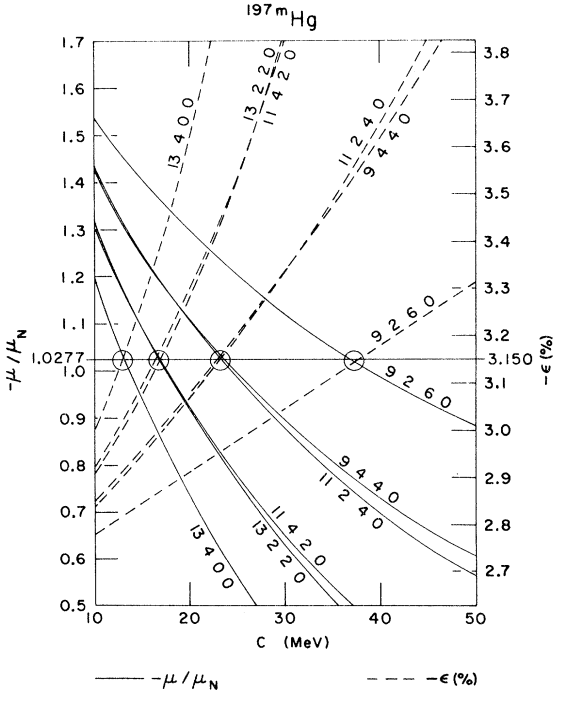

FIG. 6. Configuration-mixing predictions for the magnetic moment μ and hfs anomaly ϵ of ^{197m}Hg. C is a parameter proportional to the neutron-pairing energy.

different l is not important except in so far as it indicates the order of filling. It enters the anomaly calculation only through terms for which $\Delta l = \pm 2$. As stated, these are small except for the unlikely case of an accidental near degeneracy. For this reason the terms with $\Delta l = \pm 2$ are omitted.

1. Spin $\frac{13}{2}$

A wide variety of configurations were used to calculate both μ and ϵ as functions of C for the spin $\frac{13}{2}$ isomeric states of four mercury isotopes. A reasonable selection of these is shown in Figs. 6–9. In Fig. 6 the various configurations are seen to predict the experimental magnetic moment $-\mu/\mu_N = 1.0277$ of ^{197m}Hg for a variety of different C values. However, if for a particular configuration the same value of C which gives the experimental μ is used to predict the corresponding ϵ, one obtains $-\epsilon \cong 3.15\%$ for each of the given configurations. This fact has been used in Fig. 6 to translate the ϵ scale so that this value of ϵ coincides with the experimental μ. This scale position is for convenience only. Corresponding configurations are circled at the experimental μ value as an aid to identification. The fact that each of the configurations gives $-\epsilon \cong 3.15\%$ for the appropriate value of C indicates that the predictions of

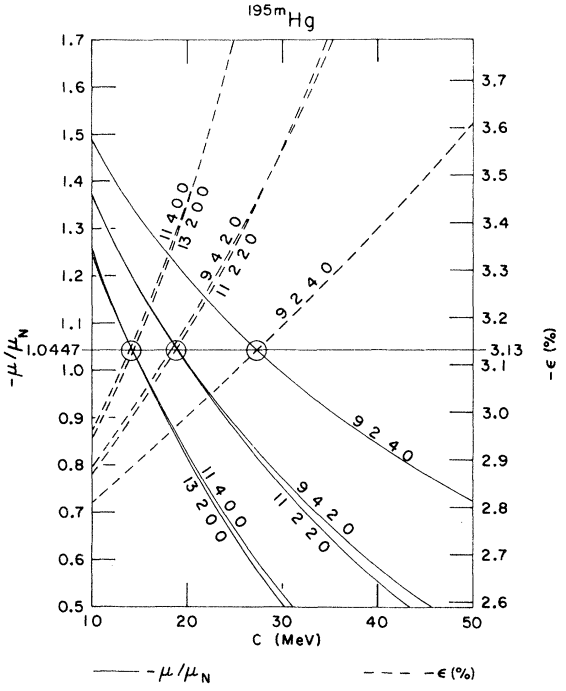

FIG. 8. Configuration-mixing predictions for the magnetic moment μ and hfs anomaly ϵ of ^{195m}Hg. C is a parameter proportional to the neutron-pairing energy.

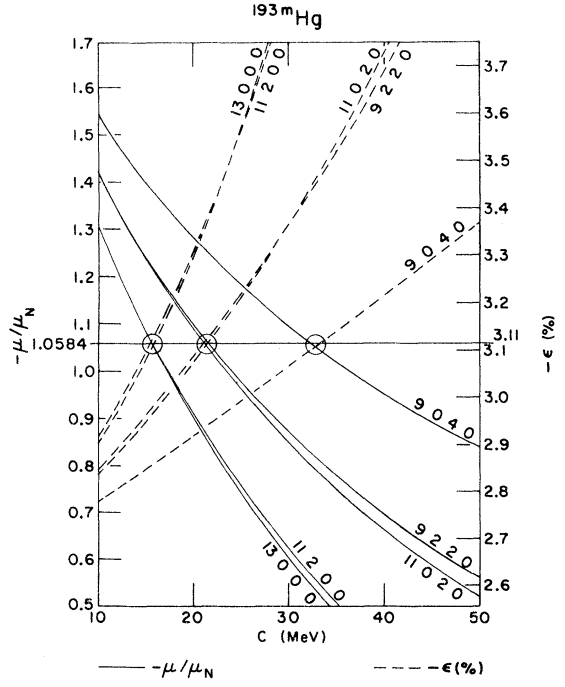

FIG. 7. Configuration-mixing predictions for the magnetic moment μ and hfs anomaly ϵ of ^{193m}Hg. C is a parameter proportional to the neutron-pairing energy.

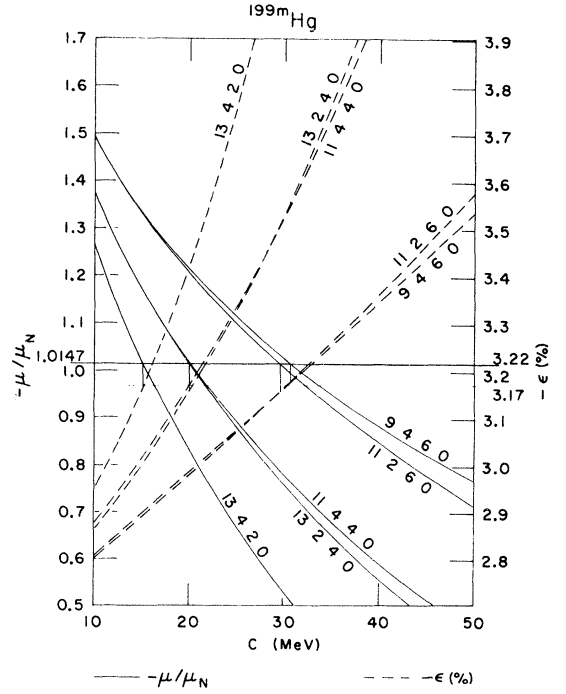

FIG. 9. Configuration-mixing predictions for the magnetic moment μ and hfs anomaly ϵ of ^{199m}Hg. C is a parameter proportional to the neutron-pairing energy.

μ and ϵ are not completely independent tests of a particular configuration.

The configuration-mixing model with a δ-function interaction does not give corrections to μ or ϵ for ground-state configurations having a single neutron in a $p_{1/2}$ state. The ground state of ^{199}Hg, however, has been noted[40] to be rather poorly described by any simple shell model. The shell-model ground state, for example, is predicted to be $I=\frac{5}{2}$. Consequently it was decided to fix $\epsilon(199)$ empirically. This can be done in a consistent manner by assuming $-\epsilon(197m)=3.150(5)\%$ as indicated in Fig. 6 and then using the experimental value $_{197m}\Delta_{199}(s_{1/2})=1.132(11)\%$ to calculate $-\epsilon(199)=4.282(12)\%$. All other "experimental" anomalies were then calculated with this value for $\epsilon(199)$ and the appropriate differential anomalies $_x\Delta_{199}(s_{1/2})$.

The success of this approach is shown in Figs. 7, 8, and 9. In each case the scale for ϵ has been shifted so that the experimental ϵ coincides with the experimental value of μ/μ_N. As is apparent the value of C which gives the experimental moment also closely predicts the correct anomaly for ^{193m}Hg, ^{195m}Hg, and ^{199m}Hg.

It is interesting to see if possible configurations for the different isomers can be grouped into families which predict μ and ϵ well and have a simple progression of occupation numbers and similar C's. A family having 13 neutrons in the $1i_{13/2}$ level and another with 11 neutrons, except for ^{199m}Hg which has 13, are seen to be suitable and are listed in Table VI. The average value of C which gives agreement between the theoretical and experimental μ is 15.0 MeV in the first case and 16.6 MeV in the second. In turn, the use of these average C's for each configuration in their respective families predicts μ within 8% and ϵ within 3% of the experimental values.

However, the use of a common C for the different isomers is questionable since the C's determined from the binding energies, C_{BE}, vary from 25 to 34 MeV. As in the case of other nuclei, the direct use of C_{BE} does not give good agreement. The above suggested families correctly predict μ and ϵ for C's which are about half of the respective C_{BE}'s.

2. Spin $\frac{5}{2}$

The choice of the neutron configuration $\nu(1i_{13/2})^{14}(3p_{3/2})^4(2f_{5/2})^5(3p_{1/2})^0$ for ^{203}Hg gives agreement with the experimental μ for $C=35.7$ MeV, whereas $C_{BE}=53.5$ MeV. Any other configuration for ^{203}Hg requires $C>55$ MeV. Also, since ^{205}Hg has spin $\frac{1}{2}$ it is very likely that its configuration

TABLE VI. Comparison of experimental and theoretical results for ϵ as predicted by the nuclear configuration-mixing model. The unperturbed neutron configuration is $\nu(1i_{13/2})^w(3p_{3/2})^x(2f_{5/2})^y(3p_{1/2})^z$ and the choice $\epsilon(199)=-4.282\%$ is made.

Spin	Isotope	Occupation numbers w	x	y	z	C_{BE} (C from binding energies) (MeV)	C_μ (C from μ_{exp}) (MeV)	$-\epsilon$ (ϵ for $C=C_\mu$) (%)	$-\epsilon$ "Experimental" value (%)
$\frac{13}{2}$	193m	13	0	0	0	33.5	15.6	3.11	3.11
	195m	13	2	0	0	34.2	14.3	3.13	3.13
	197m	13	4	0	0	32.1	13.2	3.150	3.150
	199m	13	4	2	0	25.1	15.1	3.17	3.22
	193m	11	2	0	0	33.5	15.6	3.11	3.11
	195m	11	2	2	0	34.2	19.0	3.13	3.13
	197m	11	4	2	0	32.1	16.8	3.150	3.150
	199m	13	4	2	0	25.1	15.1	3.17	3.22
$\frac{5}{2}$	203	14	4	5	0	53.5	35.7	3.33	3.40
$\frac{3}{2}$	193	12	1	0	0	54.5	46.1	2.46	3.60
	201	12	3	6	0	42.9	26.1	2.67	4.12
	201	14	3	4	0	42.9	19.8	2.67	4.12

Spin	Isotope	Single-particle predictions μ/μ_N	$-\epsilon$ (%)	$-\epsilon$ from experimental μ (%)	$-\epsilon$ "Experimental" (%)
$\frac{1}{2}$	195	+0.638	3.45	4.07	4.12
	197	+0.638	3.48	4.17	4.20
	199	+0.638	3.43	4.33	4.282

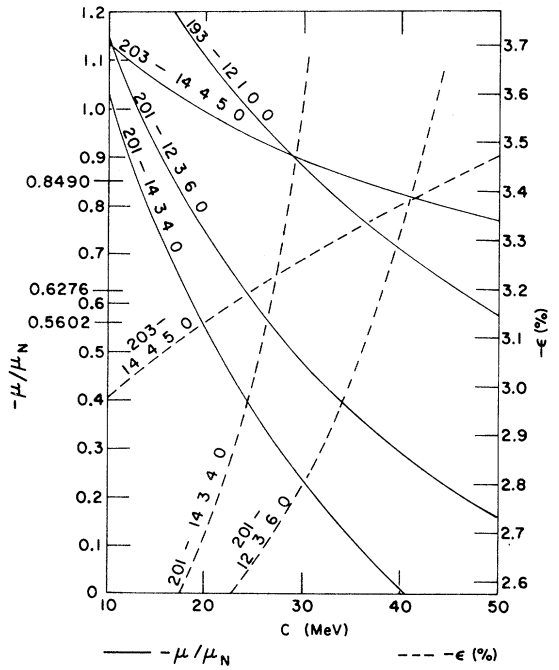

FIG. 10. Configuration-mixing predictions for the magnetic moments μ and hfs anomalies ϵ of ^{193}Hg, ^{201}Hg, and ^{203}Hg. C is a parameter proportional to the neutron-pairing energy.

is $\nu(1i_{13/2})^{14}(3p_{3/2})^4(2f_{5/2})^6(3p_{1/2})^1$ from which the above choice for ^{203}Hg follows naturally. Furthermore, the corresponding prediction of ϵ is lower than the experimental value by a factor of less than 3%. Plots associated with this configuration appear in Fig. 10 and values are given in Table VI.

3. Spin $\frac{9}{2}$

The most likely candidate for the configuration of ^{193}Hg is $\nu(1i_{13/2})^{12}(3p_{3/2})^1(2f_{5/2})^0(3p_{1/2})^0$. With this configuration the experimental value of μ is obtained for $C = 46.1$ MeV, whereas $C_{\mathrm{BE}} = 54.5$ MeV. However, the corresponding prediction of ϵ is unreasonably small. Similarly, the $\nu(1i_{13/2})^{14}(3p_{3/2})^3(2f_{5/2})^4(3p_{1/2})^0$ and $\nu(1i_{13/2})^{12}(3p_{3/2})^3(2f_{5/2})^6(3p_{1/2})^0$ configurations for ^{201}Hg lead to correct predictions of μ for respective C's of 19.8 and 26.1 MeV, whereas $C_{\mathrm{BE}} = 42.7$ MeV. The corresponding predictions of ϵ are 35% too small. Apparently, a more reasonable ϵ can be obtained only by assuming a higher value for C, in which case the prediction of μ is compromised. The dependence of μ and ϵ on C for these configurations is shown in Fig. 10. Numerical values are given in Table VI.

4. Spin $\frac{1}{2}$

As was already mentioned, there are no corrections to the single-particle prediction of μ or ϵ when the odd neutron is in a $p_{1/2}$ state. Therefore, one obtains $\mu = +0.638\mu_N$, independent of C, for all of the isotopes with $j = \frac{1}{2}$ ground states. This μ is about 20% too large, and if it is used in the calculation of ϵ the results are about 20% too small. However, the use of the experimental values of μ in the calculation of ϵ gives magnitudes which agree within 1%.

5. Summary

The results given in Table VI show that the configuration-mixing predictions for μ and ϵ for $I = \frac{13}{2}$ mercury isomers are quite good if one assumes a constant strength parameter C which is about half the value calculated from the binding energies. If one uses the C which gives the experimental value of μ for $I = \frac{5}{2}$ ^{203}Hg, the resulting ϵ is also close to the experimental value. It appears impossible to predict reasonable values of both μ and ϵ with a given C for $I = \frac{3}{2}$ isomers. Spin $I = \frac{1}{2}$ isomeric states are unaffected by configuration mixing with a δ-function interaction but good values of ϵ are obtained when calculated from the experimental values of μ. In order to increase the precision of the predicted values significantly a different nuclear model more specifically tailored to mercury is probably required.

ACKNOWLEDGMENTS

Thanks are due George Moe for the development of the signal averaging program and associated computer hardware. C. C. Chan has aided in recovering the radioactive mercury and accumulating data. Bruce Geelhood provided the necessary modifications of a computer program to obtain the values of $A(^3P_1)$. The staff of the physics shop under the supervision of Weldon Pursel have been very helpful. Glassblowers Robert Morley and Jacob Jonson deserve special thanks for all the quartzware they have assembled. Finally, the University of Washington cyclotron staff under the direction of Dr. William Weitkamp are thanked for the target irradiations – especially Barbara Lewellen for her steady hand at the controls of the cyclotron and Jack Orth for his aid in emergency maintenance.

*Research supported in part by the National Science Foundation.

[1]B. Cagnac, Ann. Phys. (Paris) **6,** 467 (1961).
[2]W. T. Walter, Massachusetts Institute of Technology Research Laboratory of Electronics Quarterly Progress Report No. 62, July 15, 1961 (unpublished), p. 105.
[3]W. T. Walter, Ph.D. thesis, Massachusetts Institute of Technology, 1962 (unpublished).
[4]J. C. Lehmann and R. Barbé, C.R. Acad. Sci. (Paris) **257,** 3152 (1963).
[5]M. J. Stavn, Bull. Am. Phys. Soc. **9,** 10 (1964).
[6]O. Redi, Phys. Lett. **31B,** 567 (1970).
[7]P. A. Moskowitz, C. H. Liu, G. Fulop, and H. H. Stroke, Phys. Rev. C **4,** 620 (1971).
[8]J. Bonn, G. Huber, H. J. Kluge, U. Kopf, L. Kugler, and E. W. Otten, Phys. Lett. **36B,** 41 (1971).
[9]R. H. Kohler, Phys. Rev. **121,** 1104 (1961).
[10]C. V. Stager, Phys. Rev. **132,** 275 (1963).
[11]W. W. Smith, Phys. Rev. **137,** A330 (1965).
[12]O. Redi and H. H. Stroke, Phys. Rev. A **2,** 1135 (1970).
[13]R. A. Sorenson, Am. J. Phys. **35,** 1078 (1967).
[14]R. J. Reimann, C. C. Chan, and M. N. McDermott, Bull. Am. Phys. Soc. **15,** 1509 (1970).
[15]R. J. Reimann, C. C. Chan, and M. N. McDermott, Bull. Am. Phys. Soc. **16,** 532 (1971).
[16]C. L. Braga and M. D. Lumb, J. Sci. Instrum. **43,** 341 (1966).
[17]R. L. Chaney, Ph.D Thesis, University of Washington, 1969 (unpublished).
[18]W. J. Tomlinson, III, and H. H. Stroke, Nucl. Phys. **60,** 614 (1964).
[19]G. Fulop, C. H. Liu, P. Moskowitz, and H. H. Stroke, Bull. Am. Phys. Soc. **15,** 1509 (1970).
[20]R. L. Covey and S. P. Davis, Phys. Rev. C **5,** 1397 (1972).
[21]C. F. Williamson, J. P. Boujot, and J. Picard, Centre d'Etudes Nuclearies de Saclay Report No. EA-R 3042, 1966 (unpublished).
[22]R. Vandenbosch and J. R. Huizenga, Phys. Rev. **120,** 1313 (1960).
[23]E. L. Wheeler, *Scientific Glassblowing* (Interscience, New York, 1958), Chap. X.
[24]J. Lange and H. Münzel, Karlsruhe Nuclear Research Center Report No. KFK-767, May 1968 (unpublished) [translated from German **ORNL** Report No. **ORNL**-tr-3020].
[25]A. H. Wapstra and N. B. Gove, Nucl. Data **A9,** 303 (1971).
[26]V. J. Ehlers, Y. Kabaskal, H. A. Shugart, and O. Tezer, Phys. Rev. **176,** 25 (1968).
[27]C. Cohen-Tannoudji, Ann. Phys. (Paris) **7,** 423 (1962).
[28]C. Cohen-Tannoudji, Ann. Phys. (Paris) **7,** 469 (1962).
[29]J. Dupont-Roc, N. Polonsky, C. Cohen-Tannoudji, and A. Kastler, C.R. Acad. Sci.(Paris) **B264,** 1811 (1967).
[30]W. Happer and B. S. Mathur, Phys. Rev. **163,** 12 (1967).
[31]B. A. Mamyrin, N. N. Arujev, and S. A. Alekseenko, in *Atomic Masses and Fundamental Constants,* edited by J. H. Sandars and A. H. Wapstra (Plenum, New York, 1972), Vol. 4.
[32]F. D. Feiock and W. R. Johnson, Phys. Rev. Lett. **21,** 785 (1968).
[33]These unpublished corrections were calculated by Bruce Geelhood of this laboratory. Details are included in a forthcoming publication.
[34]A. Lurio, M. Mandel, and R. Novick, Phys. Rev. **126,** 1758 (1962).
[35]A. Lurio, Phys. Rev. **142,** 46 (1966).
[36]M. N. McDermott and W. L. Lichten, Phys. Rev. **119,** 134 (1960).
[37]H. H. Stroke, R. J. Blin-Stoyle, and V. Jaccarino, Phys. Rev. **123,** 1326 (1961).
[38]A. Arima and H. Horie, Prog. Theor. Phys. **12,** 623 (1954).
[39]H. Noya, A. Arima, and H. Horie, Prog. Theor. Phys. Suppl. **8,** 33 (1958).
[40]M. B. Lewis, Nucl. Data **B6** (No. 4), 373 (1971).